Net Ecosystem Production of Dissolved Organic Carbon in a Coastal Upwelling System: The Ría de Vigo, Iberian Margin of the North Atlantic

X.A Álvarez–Salgado[1], J. Gago[1], B.M. Míguez[2], and F.F. Pérez[1]

[1] CSIC, Instituto de Investigacións Mariñas, Eduardo Cabello 6, 36208–Vigo, Spain

[2] Facultad de Ciencias del Mar, Universidad de Vigo, apartado 874, 36200–Vigo, Spain

running head: *NEP of DOC in a coastal upwelling area*

Version: 1 August 2000

Abstract

Net ecosystem production (*NEP*) rates of dissolved organic carbon (DOC) are estimated in a coastal upwelling system. The study site is a large coastal inlet (2.76 km^3) in the northern boundary (42–43°N) of the Eastern North Atlantic upwelling system. The 2–D circulation pattern in the system is governed by an offshore Ekman transport quite variable in magnitude and direction. A mass balance of the short–time–scale (2–4 days) changes in measured DOC profiles is performed to obtain the *NEP* rates. Microbial oxidation of imported labile DOC (8% of total DOC, recycling time τ <5 days) at a maximum net rate of –37 mmol C m^{-2} d^{-1} occurred during a downwelling episode in the middle of the highly productive spring period. On the contrary, extensive export of labile DOC (<15% of total DOC, τ <7 days) produced at net rates >42 mmol C m^{-2} d^{-1} took place during an upwelling episode in July, the middle of the upwelling season. This rate represents ~20% of the net primary production, demonstrating in the field the relative importance of horizontal offshore transport of labile DOC to the export of new production in upwelling systems. An autumn wind relaxation period results in dramatic changes in DOC standing stocks (± 9 µmol C L^{-1}) caused by a conspicuous time segregation between sustained net phytoplankton production of labile DOC (+15 mmol C m^{-2} d^{-1}, 11 days) and subsequent rapid bacterial degradation (–63 mmol C m^{-2} d^{-1}, 3 days). Net horizontal export during this period was prevented by reduced offshore Ekman transport values, indicating that net DOC production is not always synonymous with net export. Finally, during the winter period, the large wind–driven net DOC horizontal exchange rates affected mainly the DOC standing stocks of no bioreactive materials in the system, whereas bacterial oxidation rates during this period reduced to less than –0.14 mmol C m^{-2} d^{-1}.

Acknowledgements

The authors thank the captain and crew of '*R/V Mytilus*' and the members of the IIM Group of Oceanography for their help during the sampling programme. M.V. González assisted us in the preparation of figures. Comments by K. Soetaert have contributed to improve the manuscript. Financial support for this work came from CICYT Grant No. AMB95−1084. Fellowships from the Spanish 'Ministerio de Educación y Ciencia' funded J. Gago and B. Míguez to carry out this work.

Introduction

Incorporation of the phytogenic bioreactive fractions of dissolved organic matter (DOM) in experimental (Carlson et al. 1994) and modelling (Anderson and Williams 1999) approaches to carbon cycling have advanced our understanding of the fate of primary production in the oceans. The bioreactive DOM with recycling times shorter than residence times in the study system —the labile fraction— will contribute to the regenerated production. The dimensions of the system (local to global) will dictate the time–scales (days to months) involved. The bioreactive DOM with recycling times larger than residence times —the semilabile fraction— will contribute to the export production, which equals new production under steady state conditions. Therefore, the early Eppley and Peterson's (1979) concept of new production has been revisited because of the major contribution of DOM to organic matter export (Bronk et al. 1994).

Local downward export during winter mixing is the fate of semilabile DOM accumulated in the surface layer of areas where convective mixing succeeds summer stratification. This is the case of the NW Mediterranean (Copin–Montégut and Avril 1993) or the Sargasso Sea (Carlson et al. 1994). In contrast, horizontal transport of semilabile DOM occurs from the eutrophic Equatorial Pacific to the adjacent oligotrophic subtropical gyres (Hansell and Waterhouse 1997). Intensified horizontal flows in ocean margins must contribute significantly to the export of shelf primary production towards the adjacent ocean via semilabile DOM. Therefore, bioreactive DOM has to be incorporated in the unclosed controversy about the relative importance of export and *in situ* oxidation of organic matter produced in continental shelves (e.g. Walsh et al. 1988; Biscaye et al. 1994). Primary production and export of phytogenic materials are enhanced in coastal upwelling regions, in response to the magnified

shelf–edge exchange caused by the offshore Ekman transport (Walsh 1991; Wollast 1993).

Despite their relevance to global productivity and export, few studies have been conducted on the role of bioreactive DOM in coastal upwelling areas. In fact, these studies are circumscribed to the western coast of the Iberian Peninsula, the northern limit of the NW Africa upwelling system (Doval et al. 1997; Álvarez–Salgado et al. 1999). The Rías Baixas —four large V–shaped indentations there— constitute a unique 'macrocosms' to study the short–time–scale response of the carbon cycle to shelf wind–stress. The Ekman transport controls the extremely variable short–time–scale 2–D circulation pattern of the Rías Baixas (Rosón et al. 1997), either during the upwelling (April–October) or the downwelling favourable (November–March) seasons (Wooster et al. 1976; Bakun and Nelson 1991). The inorganic carbon and nutrients balances for the entire ecosystem are also subject to Ekman transport control (Pérez et al. 2000). The recent studies of Doval et al. (1997) and Álvarez–Salgado et al. (1999) describe the Rías Baixas as the pre–eminent site of formation for the bioreactive DOM excess observed in shelf surface waters during the upwelling season.

The present work complements the previous studies on the seasonal variation of DOM by focusing on the short–time–scale (½ wk) changes in the net ecosystem production (NEP) of bioreactive dissolved organic carbon (DOC) in the Ría de Vigo (NW Spain). The relative importance of accumulation *vs* export under contrasting hydrographic conditions during four seasons will be examined in detail. NEP of bioreactive DOC —i.e. the DOC balance of production minus consumption for the entire ecosystem (Smith and Hollibaugh 1997)— will be estimated with a biogeochemical box–model successfully applied to the adjacent Ría de Arousa (e.g. Pérez et al. 2000).

Material and Methods

The sampling programme

An intensive hydrographic sampling was executed in the Ría de Vigo during four contrasting periods in 1997: 7–23 April, 1–18 July, 15 September–2 October, and 1–11 December. Five fixed stations were occupied, four along the main axis of the embayment and one at the shallower entrance, north of the Isles Cies (Fig. 1). Full–depth continuous conductivity–temperature–depth profiles were recorded at each sampling site with a SBE 25 CTD device. Conductivity measurements were converted into practical salinity scale values (UNESCO 1985). Subsequently, seawater samples for salinity analysis with an Guideline AUTOSAL 8400A and DOC determination with a Shimadzu TOC–5000 analyser were collected from 3–5 depths with 5 litre Niskin bottles. This programme was repeated every 2–4 days during the four sampling periods, the appropriate frequency to study the coupling between meteorological forcing and hydrography at the short–time–scale (Rosón et al. 1997). A total of 22 surveys were performed: 6 during the spring, summer and autumn, and 4 during the winter period.

Daily Ekman transport values ($-\overline{Q}_X$) have been calculated according to Wooster et al. (1976):

$$-Q_X = \frac{\rho_{air} \cdot C \cdot |V| \cdot V_N}{\rho_{sw} \cdot f} \qquad (1)$$

Where ρ_{air} is the density of air, 1.22 kg·m^{-3} at 15°C; C is an empirical drag coefficient (dimensionless), 1.3·10^{-3}; f is the Coriolis parameter, 9.946·10^{-5} s^{-1} at 43° latitude; ρ_{SW} is the density of seawater, ~1025 kg·m^{-3}; $|V|$ is wind speed; and V_N is the north component of wind speed. Wind data were taken at the Cape Finisterre Meteorological Observatory.

DOC determination by high temperature catalytic oxidation

Samples for the analyses of DOC were collected into 250 ml acid–cleaned all–glass flasks. They were immediately filtered through 47 mm ∅ Whatman GF/F filters (ashed 450°C, 4 hours) in an acid–cleaned all–glass filtration system, and collected in 10 ml glass ampoules (ashed 450°C, 12 hours). After acidification with H_3PO_4 to pH <2, the ampoules were heat–sealed and stored in the dark at 4°C, until analysed in the laboratory. DOC content in samples was measured with a commercial Shimadzu TOC–5000 organic carbon analyser, working under the principle of high temperature catalytic oxidation. After decarbonation of the sample by vigorous stirring with high purity synthetic air for 15 min, 200 µl were injected into the vertical furnace of the analyser, filled with a conditioned 0.5% Pt coated Al_2O_3 catalyst at 680°C. Conditioning consisted of washing the catalyst by repetitive injections of Milli–Q water, until the blank was low and stable. Quantitative production of CO_2 occurs from the dissolved organic carbon (DOC) in the sample. High purity synthetic air carries the combustion products through a series of scrubbers (25% H_3PO_4 solution, in–built Peltier cooler at ~1°C, halogen scrubber and particle filter) before the dried gas mixture enters the measuring cell of the Shimadzu Infra–red gas analyser. The system was standardised daily with potassium hydrogen phthalate in milli–Q water. The concentration of DOC was determined by subtracting the system blank area from the average peak area and dividing by the slope of the standard curve. The system blank —obtained by frequent injection (every 4–6 samples) of UV–Milli–Q water— was equivalent to 5–10 µmol C L^{-1}. The precision of measurements was <1%, *i.e.* ±0.5 µmol C L^{-1}. The accuracy of our DOC measurements were tested daily with the TOC reference materials provided by J. Sharp (University of Delaware) with very satisfactory results. We obtained an average concentration of 45.4±1.1 µmol C L^{-1} (n = 44) for the

DEEP OCEAN reference (Sargasso Sea deep water, 2600 m) and 0.4±0.7 µmol C L^{-1} (n= 44) for the BLANK reference material. The nominal values provided by the reference laboratories are 44.0 ±1.5 and 0.0±1.5 µmol C L^{-1} respectively.

Estimation of the NEP of DOC with a 2–D box model

The transient 2–D mass–heat weighted box model used by Rosón et al. (1997) in the adjacent Ría de Arousa has been adapted to the Ría de Vigo. The box model estimates the average residual exchange fluxes (horizontal and vertical advection, vertical mixing) which produce the salinity and temperature changes observed in the embayment between two consecutive surveys, separated 2–4 days. For the purposes of this work, only the horizontal advective fluxes will be considered. Table 1 defines the relevant terms of the model used throughout the text.

Two boundaries are defined, which delimit the study system (Fig. 2). The inner limit separates the ría from San Simón Bay, the estuary of the river Oitabén–Verdugo. The outer limit separates the ría from the continental shelf off the Rías Baixas. Each boundary consists of two layers (surface and bottom), flowing in opposite directions. The level of no–horizontal motion between the surface and bottom layer is the gravity centre of the boundary, *i.e*. the depth at which the actual density coincides with the average density of the boundary (Rosón et al. 1997). The average salinity and temperature of the surface and bottom layer of each boundary and box are obtained by integration of the calibrated CTD profiles. For each boundary we can define the average flux of surface water ($\overline{Q_S}$, m^3 s^{-1}), salt ($\overline{Q_S \cdot S_S}$, kg s^{-1}) and heat ($\overline{Q_S \cdot T_S}$, °C m^3 s^{-1}) between two consecutive surveys. Equations for volume, salt and heat conservation can be written for the segment delimited within the boundary: San Simón Bay for the case of boundary 1 and the ría+San Simón bay for the case of boundary 4 (Fig. 2).

$$\overline{Q_S} = \overline{Q_B} + \overline{R} \tag{2}$$

$$V \cdot \frac{\Delta S}{\Delta t} = \overline{Q_B \cdot S_B} - \overline{Q_S \cdot S_S} \tag{3}$$

$$V \cdot \frac{\Delta T}{\Delta t} = \overline{R \cdot T_R} + \overline{H} + \overline{Q_B \cdot T_B} - \overline{Q_S \cdot T_S} \tag{4}$$

Where $\overline{R}$ ($m^3\ s^{-1}$) and $\overline{R \cdot T_R}$ (°C $m^3\ s^{-1}$) are the average water and heat fluxes due to continental runoff between two consecutive surveys. $\overline{H}$ (°C $m^3\ s^{-1}$) is the average air–sea heat exchange flux across the sea surface of the segment delimited within the boundary between two consecutive surveys. V (m^3) is the volume of the segment limited within the boundary. $\frac{\Delta S}{\Delta t}$ (kg $m^{-3}\ s^{-1}$) and $\frac{\Delta T}{\Delta t}$ (°C s^{-1}) are the average salinity and temperature change on the segment delimited by the boundary between two consecutive surveys. $\overline{Q_B}$ ($m^3\ s^{-1}$), $\overline{Q_B \cdot S_B}$ (kg s^{-1}) and $\overline{Q_B \cdot T_B}$ (°C $m^3\ s^{-1}$) are the average fluxes of water, salt and heat in the bottom layer between two consecutive surveys. It should be noticed that $\overline{R}$, $\overline{H}$, V, $\frac{\Delta S}{\Delta t}$ and $\frac{\Delta T}{\Delta t}$ refer to the drainage basin, the surface area and the volume of San Simón Bay for the case of boundary 1 and of the ría+San Simón Bay for the case of boundary 4.

Two reasonable assumptions are implicit in the system of equations: **1**) the volume of the ría is constant; and **2**) the contribution of the *P–E* term to the water budget is negligible. In fact, the *P–E* term was calculated to verify its minor contribution. Another less–obvious assumption is that horizontal mixing can be ignored. The horizontal circulation in the ría is controlled by shelf wind–stress, which produces enhanced advection. Horizontal velocities are normally >3 10^{-2} m s^{-1}, whereas turbulent diffusion coefficients are around 10 $m^2\ s^{-1}$ (Rosón et al. 1997). Considering these

numbers and the observed DOC gradients in the ría (Figs 3, 5, 6 and 7), the contribution of horizontal mixing to net DOC fluxes is usually <5%.

The extreme variability of water fluxes compared with salinity and temperature changes between two consecutive surveys allows the simplification of equations (3) and (4):

$$V \cdot \frac{\Delta S}{\Delta t} = \overline{Q}_B \cdot \overline{S}_B - \overline{Q}_S \cdot \overline{S}_S \tag{5}$$

$$V \cdot \frac{\Delta T}{\Delta t} = \overline{R} \cdot \overline{T}_R + \overline{H} + \overline{Q}_B \cdot \overline{T}_B - \overline{Q}_S \cdot \overline{T}_S \tag{6}$$

Two sets of water fluxes can be obtained, from the equations of water (1) and salt (5) conservation, $(\overline{Q}_S)_S$, and the equations of water (1) and heat (6) conservation, $(\overline{Q}_S)_T$:

$$(\overline{Q}_S)_S = \frac{\overline{R} \cdot \overline{S}_B + V \cdot \frac{\Delta S}{dt}}{\overline{S}_B - \overline{S}_S} \tag{7}$$

$$(\overline{Q}_S)_T = \frac{\overline{R} \cdot (\overline{T}_B - \overline{T}_R) - \overline{H} + V \cdot \frac{\Delta T}{dt}}{\overline{T}_B - \overline{T}_S} \tag{8}$$

Finally, the mass–heat weighted water flux, $\overline{Q}_S$, is estimated as:

$$\overline{Q}_S = (\overline{Q}_S)_S \cdot (1 - \overline{w}) + (\overline{Q}_S)_T \cdot \overline{w} \tag{9}$$

Where $\overline{w}$ is a dimensionless factor that weights the contribution of salinity and temperature to the density gradient, the responsible of the observed water fluxes:

$$\overline{w} = \frac{(\overline{T}_B - \overline{T}_S)^2}{(\overline{T}_B - \overline{T}_S)^2 + \left(\frac{\overline{\beta}}{\overline{\alpha}}\right)^2 (\overline{S}_B - \overline{S}_S)^2} \tag{10}$$

The ratio of the coefficients of haline contraction and thermal expansion, $\frac{\overline{\beta}}{\overline{\alpha}}$, is used to convert the salinity gradient into temperature units:

$$\frac{\overline{\beta}}{\overline{\alpha}} = \frac{\frac{1}{\rho}\cdot\left(\frac{\partial\rho}{\partial S}\right)_T}{-\frac{1}{\rho}\cdot\left(\frac{\partial\rho}{\partial T}\right)_S} \tag{11}$$

$\frac{\overline{\beta}}{\overline{\alpha}}$ was calculated from the equation of state of seawater (UNESCO 1985) for the average salinity and temperature of each boundary between t_1 and t_2.

Once water fluxes are known, the average budget of DOC outputs minus inputs ($O–I$, mol C s^{-1}) between two consecutive surveys can be calculated as:

$$\begin{aligned} O - I &= \overline{Q}_S \cdot \overline{DOC}_S - \left(\overline{Q}_S - \overline{R}\right)\cdot \overline{DOC}_B - \overline{R}\cdot\overline{DOC}_R - \overline{W}\cdot\overline{DOC}_W = \\ &= \overline{Q}_S \cdot \left(\overline{DOC}_S - \overline{DOC}_B\right) - \overline{R}\cdot\left(\overline{DOC}_R - \overline{DOC}_B\right) - \overline{W}\cdot\overline{DOC}_W \end{aligned} \tag{12}$$

Where $\overline{DOC}_B$ and $\overline{DOC}_S$ are the average concentration of DOC in the surface and bottom horizontal fluxes, and $\overline{W}$ and $\overline{DOC}_W$ are the average flux of water and the concentration of DOC in the sewage from the City of Vigo (Fig. 1). $\overline{DOC}_R$ and $\overline{DOC}_W$ are set to 400 µmol C L^{-1} and 3.6 10^3 µmol C L^{-1} respectively (Doval et al. 1997).

Finally, the average net ecosystem production of DOC, $\overline{NEP}$, in the study system is:

$$\overline{NEP} = V\cdot\frac{\Delta DOC}{\Delta t} + O - I \tag{13}$$

The box model approach might involve large potential errors in the estimation of the NEP of DOC, but it is a unique method to measure the whole–community metabolism directly (Smith and Hollibaugh 1997) and avoids most of the problems associated to *in vitro* methods: reduced turbulence, unnatural light fields, altered grazer communities... Therefore, box model estimations of rate measurements are probably

less accurate than *in vitro* techniques but the resultant values are ready for direct interpretation at the ecosystem level.

Results

The Ría de Vigo was intensively sampled during four distinct periods along 1997, looking for contrasting hydrodynamic (upwelling, downwelling) and biogeochemical (ecosystem production and respiration of DOC) conditions. The short time and space variability of the salinity, temperature and DOC profiles and the corresponding outputs from the 2–D box model (water and DOC fluxes, net DOC production and accumulation) are presented for each period. The results are appraised on the light of the response to the external forces acting on the embayment (continental runoff, offshore Ekman transport).

Spring: consumption of DOC imported from the shelf during downwelling

Shelf winds were moderate in intensity and variable in direction during the spring survey, producing offshore Ekman transport absolute values <300 $m^3\ s^{-1}\ km^{-1}$ (Fig. 3a). Continental runoff was rather low, increasing from 4 to 17 $m^3\ s^{-1}$. Since the surface layer of the outer boundary of the Ría de Vigo is ~10 km wide, the relative contribution of the offshore Ekman transport to water circulation in the embayment was ~2 orders of magnitude larger than the contribution of continental runoff.

The short–time–scale evolution of the salinity (Fig. 3b) and temperature (Fig. 3d) profiles in the middle Ría de Vigo (stn 3) reacted to the observed meteorological variability. The evolution of the 35.8 pss and 15°C isolines were parallel, showing a net entry of Eastern North Atlantic Central Water (ENACW) from the bottom shelf between 10 and 14 April that corresponds with a brief upwelling–favourable wind peak.

Subsequent wind relaxation was accompanied by dramatic withdraw of ENACW from 17 to 21 April, which was partially restored by upwelling–favourable winds at the end of the period (21–23 April). Salinity decreased and temperature increased in the surface layer along the period. The time–evolution of DOC (Fig. 3f) was parallel to salinity and temperature. The 70 µmol C L^{-1} isoline resembled ENACW displacements inferred above. In the surface layer, increasing stratification from 14 April was accompanied by DOC accumulation.

The 7–23 April average salinity (Fig. 3c), temperature (Fig. 3e) and DOC (Fig 3g) profiles along the main channel of the inlet illustrate marked spatial differences, which fit with relative location in regard to the external forces: runoff in the inner boundary and Ekman transport in the outer boundary. It is worth noting the wide DOC range, from <70 µmol C L^{-1} in upwelled ENACW colder than 14°C to >95 µmol C L^{-1} in DOC outwelled from San Simón Bay.

Figure 4a shows the cumulative surface water flux at the outer boundary of the ría, obtained with the 2–D box model. Despite the outgoing direction of the flux from 10 to 14 April and 21 to 23 April, the ría imported 1.42 km^3 of shelf surface waters during the whole period (Table 2), ~51% of its volume (2.76 km^3). On the other hand, 0.80 km^3 of San Simón Bay water were introduced in the surface layer of the ría across the inner boundary. Continental runoff and sewage contributions were negligible. The flushing time of the system was ~20 days (renewal rate, 5%·d^{-1}). The DOC surface flux at the outer boundary (Fig. 4a) compasses the water flux, denoting a net entry of 114.7 10^3 kmol C (average 81 µmol C L^{-1}) from shelf surface waters, 58.2% of the total DOC input (Table 2). San Simón Bay contributed with 79.6 10^3 kmol C (average 100 µmol C L^{-1}), 40.3% of the total input. Continental runoff and sewage from the City of Vigo were minor DOC donors, 1.5% of the total input.

The cumulative net balance of DOC outputs minus inputs (*O–I*; Fig. 4b) resembled the DOC surface flux across the outer boundary of the ría (Fig. 4a), yielding a net difference of –20.0 10^3 kmol C, *i.e.* –10% of the total input. Therefore, during the spring period the ría imported DOC, mainly from shelf surface waters at the outer boundary and San Simón Bay at the inner boundary. The cumulative *NEP* of DOC parallels the net *O–I* balance, demonstrating an in–depth short–time–scale (2–4 days) coupling between net DOC import and oxidation. The largest DOC net consumption rates, $\overline{NEP}$ = –49.8 mol C s^{-1}, occurred between 7 and 10 April (Table 3), when ~93% of the DOC which entered the ría came from shelf surface waters accompanying a strong reversal of the positive circulation in the outer boundary. During these 3 days it is oxidised ~50% of the total amount of DOC consumed along the whole 16 days period. The net *O–I* balance represents 80% of the net ecosystem consumption of DOC in the system (*NEP* = –25 10^3 kmol C). The remaining 20% came from the DOC previously accumulated in the ría ($V \cdot \Delta DOC/\Delta t$ = –5 10^3 kmol C).

Summer: export to the shelf of DOC produced during upwelling

The summer period —in the middle of the upwelling season— coincided with upwelling–favourable northerly winds that produce offshore Ekman transport values ranging between 85 and 860 m^3 s^{-1} km^{-1} (Fig. 5a). On the contrary, continental runoff was extremely low: <7 m^3 s^{-1}.

The short–time–scale evolution of the salinity (Fig. 5b) and temperature (Fig. 5d) profiles indicate water displacements in agreement with shelf winds forcing (Fig. 5a). Upwelling favourable winds from 1 to 8 July produced the entry of ENACW colder (<14°C) and saltier (>35.9 pss) than during the spring period. Wind relaxation from 8 to

11 July was accompanied by the corresponding isopleths deepening. Finally, strong upwelling favourable winds from 11 to 18 July produced the massive entry of ENACW colder than 13°C in the middle ría. DOC profiles (Fig. 5f) followed the variability of the thermohaline properties. The 70 µmol C L^{-1} isoline is parallel to the 14–15°C isopleths and DOC concentrations <60 µmol C L^{-1} were recorded for temperatures <13°C. On the other hand, DOC levels >90 µmol C L^{-1} were observed in stratified surface waters during upwelling relaxation. The average effect of upwelling on the salinity (Fig. 5c), temperature (Fig. 5e) and DOC (Fig. 5g) profiles along the main axis of the embayment can be clearly observed. Bottom water saltier than 35.8 pss, colder than 14°C and with DOC concentration <70 µmol C L^{-1} penetrated up to the shallow reaches of the inner ría.

As a result of the prevailing northerly winds over the shelf, water circulation at both the inner and outer boundaries of the ría was positive (Fig. 4c, Table 2). A volume of 4.86 km^3 of ENACW upwelled over the shelf entered the ría across the bottom outer boundary from 1 to 18 July. On the contrary, only 0.31 km^3 of San Simón Bay water entered across the surface inner boundary. The contributions of continental runoff and sewage were again negligible. The flushing time of the system during this period reduced to only 9 days (renewal rate, 11% d^{-1}) and the exchange across the outer boundary accounted for 94% of the total renewal. The circulation was particularly intensified from 11 to 18 July. In agreement with the circulation pattern, the main DOC source to the ría was the DOC–poor ENACW (average 64 µmol C L^{-1}) that represented 90.0% of the total DOC influx. DOC entering the ría from San Simón Bay (average 100 µmol C L^{-1}) amounted 8.9% of the total input (Table 2).

The cumulative *O–I* balance of DOC (Fig. 4d) yields a net difference of +47.1 10^3 kmol C, revealing that the ría was acting as a DOC source to shelf surface

waters. The cumulative *NEP* of DOC is coupled with the net *O–I* balance that, in turns, goes with the surface water flow in the outer boundary (Fig. 4a). The DOC produced within the ría at the time scale of the flushing time (τ = 9 days) represented ~80% of the total amount of DOC exported to the shelf. The exported material was produced during the vigorous upwelling episodes of 4 to 8 July and 15 to 18 July, when the *NEP* of DOC was 56.5 and 66.5 mol C s^{-1} respectively (average 60.9 mol C s^{-1}; Table 3). The lasting 20% of DOC exported to the shelf came from materials previously accumulated in the ría and involved a 5% reduction of the DOC amount in the ría at the beginning of the period.

Autumn: 'in situ' production and consumption of DOC during wind relaxation

A prolonged (>10 days) wind calm —characteristic of the transition from the upwelling– to the downwelling–favourable season (Nogueira et al. 1997)— was monitored during this period. The offshore Ekman transport ranged from –30 to 160 m^3 s^{-1} km^{-1} (Fig. 6a). Continental runoff was also quite limited: <5 m^3 s^{-1}. Under these conditions, the time evolution of the salinity (Fig. 6b), temperature (Fig. 6d) and DOC (Fig. 6f) profiles indicate a broad trend to withdraw the salty, cold and DOC–poor ENACW in the bottom layer of the middle ría. However, from 18 to 28 September the 14°C isobath pointed to a transitory re–entry of ENACW into the ría. In the surface layer, stratification increased with time and it was accompanied by a marked accumulation of DOC (>85 µmol C L^{-1}). The average salinity (Fig. 6c), temperature (Fig. 6e) and DOC (Fig. 6g) distributions along the main axis of the ría show limited haline and strong temperature and DOC gradients, similar to the observations made during the spring period (Figs. 3c, e & g).

Prolonged wind relaxation produced limited water exchange across the outer boundary of the ría through this period (Fig. 4e, Table 2). Only 17% and 28% of the volume of the ría was renewed with San Simón Bay and continental shelf surface waters, respectively. Therefore, the flushing time was extremely large: 38 days (renewal rate, 2.6% d^{-1}). Accordingly, DOC exchange fluxes were very limited compared with the spring and summer periods. Only 57.6 10^3 kmol C entered from shelf surface waters (average 74 µmol C L^{-1}) and 44.3 10^3 kmol C from San Simón Bay (average 92 µmol C L^{-1}). Continental runoff and sewage represented 0.9% and 2.5% of the total DOC input to the ría (Table 2).

Progressive accumulation of the DOC produced from 15 to 29 September, at an average *NEP* rate of +20.3 mol C s^{-1}, was observed (Fig. 4f; Table 3). By 29 September the *NEP* of DOC amounted +24.6 10^3 kmol C, which represents 83% of the total DOC accumulation. It is interesting to note that during these 11 days a slow–moving positive circulation was restored, producing a net entry of 0.45 km^3 of DOC–poor ENACW from the bottom shelf. DOC produced during this 3rd period was not exported as in the summer period, but accumulated into the ría. The remaining 17% of accumulated DOC came from the net import of extrinsic materials, accounted by the *O–I* balance. The close coupling between the surface water and DOC fluxes at the outer boundary and the *O–I* balance suggests that most of the external DOC accumulated in the system came from the shelf. The initial DOC amount into the ría at the beginning of the study period (188.4 10^3 kmol C) increased by +16% on 29 September. However, during the subsequent reversal of the circulation pattern from 29 September to 2 October ~90% of the DOC produced during the previous days was consumed at the extremely high net rate of 85.6 mol C s^{-1} (Table 3).

Winter: exchange and accumulation of DOC during the unproductive season

Dramatic changes occurred during this period in the wind regime (Fig. 7a), evolving from upwelling favourable northerly winds on 1–5 December (200 m^3s^{-1} km^{-1}) to downwelling favourable southerly winds on 8–11 December (–1500 m^3 s^{-1} km^{-1}). Continental runoff was high, ranging from 52 m^3 s^{-1} on 1–5 December to 26 m^3 s^{-1} on 8–11 December.

Time changes in the salinity (Fig. 7b) temperature (Fig. 7d) and DOC (Fig. 7f) profiles are concomitant with the wind regime, showing dramatic changes in the orientation of the isopleths (see 35.0 pss, 17.0 °C and 75 µmol C L^{-1} for reference). Despite the winter conditions, bottom waters of the ría were warm and salty, as expected in the Iberian upwelling system at this time of the year. A poleward flowing slope current of warm and salty subtropical water is usually observed (Haynes and Barton 1990). Under strong downwelling conditions these subtropical waters enters the rías, as occurs from 5 to 11 December. Downwelling was so intense that water column homogenisation in the middle ría was almost complete. This contrast with the situation observed from 1 to 5 December, when the positive circulation pattern accompanying the initial upwelling displaced the fresh and DOC–rich water from San Simón Bay to the middle ría (stn 3). The average distributions along the main axis show the westward extension of the fresh (Fig. 7c) and DOC–rich (Fig. 7g) water outwelled from San Simón Bay and the thermal homogenisation (Fig. 7e) accompanying the entry of warm subtropical surface waters from the shelf.

Intense positive circulation occurred at the outer boundary of the ría at the beginning of this period (Fig. 4g). Water exchange with the adjacent shelf, at the extremely high average rate of 7.6 10^3 m^3 s^{-1} from 1 to 5 December, equalled the whole volume of the ría. However, from 5 to 11 December a dramatic reversal of the

circulation pattern accompanied the dominant downwelling–favourable southerly winds. As much as 5.50 km^3 entered the ría across the surface outer boundary, reintroducing twice the volume exported during the initial upwelling episode. Consequently, for the whole period the ría imported 2.36 km^3 of shelf surface water (Table 2), *i.e*. 86% of its volume. The flushing time during this period was 11 days (renewal rate, 9% d^{-1}). DOC fluxes followed the circulation pattern (Fig. 4g, Table 2), with 193.6 10^3 kmol C (average 82 µmol L^{-1}) entering the surface outer boundary (88.6%) and 17.2 10^3 kmol C (average 85 µmol L^{-1}) entering the surface inner boundary (7.9%). Continental runoff and sewage represented 2.8% and 0.7% of the total DOC input, respectively.

The *O–I* balance of DOC (Fig. 4h) was again parallel to the water and DOC fluxes across the surface outer boundary, in such a way that 11.7 10^3 kmol C of DOC were exported to the shelf between 1 and 5 December whereas 24.3 10^3 kmol C were imported from 5 to 11 December (Table 3). Short–time–scale changes in the accumulation term ($V \cdot \Delta DOC/\Delta t$) were opposite to the *O–I* balance. Export to the shelf during the initial upwelling episode reduced the DOC content of the ría and import during the subsequent downwelling episode restored the previous deficit. The total reduction of the DOC content of the ría from 1 to 5 December was due to export (64%) and oxidation (36%) at an average $\overline{NEP}$ of –18.6 mol C s^{-1} (Table 3). On the other hand, 23% of the DOC imported from shelf surface waters between 5 and 11 December was oxidised at an average $\overline{NEP}$ of –10.9 mol C s^{-1} and 77% accumulated into the ría. It is worth noting that the net DOC consumption rates by the community of organisms within the ría were much lower than during the spring downwelling episode ($\overline{NEP}$ = –49.8 mol C s^{-1}). As a consequence, the *O–I* balance of DOC was coupled with the

oxidation term (*NEP*) during the spring and with the accumulation term ($V \cdot \Delta DOC / \Delta t$) during the winter.

Discussion and conclusions

The four contrasting survey periods present exemplar hydrographic and biogeochemical situations for the NW Iberian Peninsula, the northern boundary of the coastal upwelling system that associates to the Canary Current (Bakun and Nelson 1991). The Iberian margin system has similarities with the other three major eastern boundary current regions of the World Ocean —California, Benguela and Perú/Humboldt— at comparable latitudes: off Oregon, Republic of South Africa and Chile respectively. The study site allowed us to learn about DOC cycling in a coastal upwelling area within an easily–accessible coastal inlet where exchange fluxes can be readily approached and the sampling programme is not disturbed by stormy wind conditions.

Quality of DOC produced/consumed by the community of organisms

The spring situation illustrates the rapid consumption —at the time–scale of the sampling frequency (2–4 days)— of the DOC imported by the system under downwelling conditions. From 7 to 10 April, imported DOC is consumed at the high average net rate of –0.37 mmol C m^{-2} d^{-1}. Considering the flushing time for this short event (~5 days), the consumed material has to be judged as labile DOC. Although this material represents a minor (~8%) fraction of the total amount of DOC imported by the ría, it fuels the intense bacterial activity associated to the estimated net consumption rate.

Labile DOC was probably formed in the ría and exported to the shelf during an upwelling episode on the previous days (offshore Ekman transport +0.5 10^3 m^3 s^{-1} km^{-1} for 3–6 April), being reintroduced into the embayment during the 7–10 April downwelling event. Mid February to early April is a time of intense net primary production in the study area due to the concurrency of the onset of both the spring bloom and the upwelling–favourable season (Nogueira et al. 1997). Intense net primary production enhances microbial production (exudation, grazing) of labile DOC (Norrman et al. 1995), which can be subsequently consumed by bacteria under favourable conditions for their growth. Downwelling episodes, when the nitracline deepens well below the 1% of PAR, seem to favour the succession from net production to net respiration regimes in coastal upwelling areas (Pérez et al. 2000). Nutrient depletion affects both phytoplankton and bacterial net growth (Thingstad et al. 1997), but the excess of labile DOC activates bacterial respiration. In fact, the efficiency of conversion of labile DOC into bacterial biomass reduced from 30–50% in nutrient–rich to <5% in nutrient–limited systems (Kirchman et al. 1991; Fuhrman 1992).

In contrast to the spring survey, the summer situation typifies the extensive production of labile DOC under the phytoplankton–dominated regime characteristic of upwelling conditions. Net DOC production exceeded +42 mmol C m^{-2} d^{-1} during the intense upwelling episodes of 4–8 and 15–18 July. Average flushing times in the system for these episodes were <7 days. Average net primary production in the ría during the April–October 'upwelling season' is 100–125 mmol C m^{-2} d^{-1}. It increases to >250 mmol C m^{-2} d^{-1} during upwelling episodes, when the nitrate–rich ENACW is promoted to surface waters (Moncoiffé et al. 2000). Primary production rates are similar in other coastal upwelling systems of the World Ocean (Wollast 1993). Therefore, it is expected that about 20% of the net primary production in the ría transforms into exportable DOC

under upwelling conditions. This percentage is within the 10–40% range observed in the Equatorial Pacific and other eutrophic systems (Hansell and Carlson 1998). For comparison, these authors obtain percentages of 59–70% during the spring bloom in the oligotrophic Sargasso Sea. Our percentage is also within the range of many DOC excretion for phytoplankton in coastal areas, 0–30% (Norrman et al. 1995).

The sustained DOC production of +15 mmol C m^{-2} d^{-1} from 15 to 29 September was associated with slow positive circulation provoked by weak coastal upwelling. Such circulation pattern has to produce the gently injection of nutrients into the surface layer of the ría that supports the primary production rates responsible for the estimated DOC production. The observed thermal stratification, shallow mixed layer, and limited nutrient input through weak upwelling are all favourable to the onset of red–tide assemblages (Cullen et al. 1982; Chang and Carpenter 1985). In fact, red–tides use to occur in the Iberian upwelling system at the end of the upwelling season (Figueiras and Ríos 1993) in response to increased stratification, as in other upwelling regions (Barber and Smith, 1981). The flushing time in the period 18–29 September is as high as 2 months, which causes the rapid accumulation of the produced DOC. The lability of the accumulated material is confirmed by the extensive consumption of this pool during the reversal of the circulation occurred from 29 September to 2 October. The change in the circulation pattern causes the sudden succession from phytoplankton–dominated to bacteria–dominated regimes and the accumulated labile DOC was consumed at the extremely high net rate of –63 mmol C m^{-2} d^{-1}. This net consumption rate is almost twice the rate observed during the spring survey. Lability of the materials and/or bacterial activity can be the causes behind the difference. In this sense, surface temperatures were <15.5°C in the spring episode and >17.5°C in the autumn episode.

Most of the DOC exchange between the ría and the adjacent shelf during the winter survey is coupled with the accumulation term ($V \cdot \Delta DOC / \Delta t$). This is in clear contrast with the coupling between production and export during upwelling episodes (summer) and between respiration and import during downwelling episodes (spring). DOC exchanged across the outer boundary of the ría has recycling times longer than the average 1–11 December flushing time in the study volume (11 days), and must be considered semilabile. Net DOC respiration rates during this period are <14 mmol C m^{-2} d^{-1}, i.e. <1/3 of the rate recorded during the consumption of imported labile DOC in spring. Limited production of labile materials seems to be the reason behind these low respiration rates. The average 1987–93 December–February nitrate in the surface waters of the ría is ~7 µmol N L^{-1} and Chlorophyll is <1 mg m^{-3} (Nogueira et al. 1997) which indicates reduced net primary production rates. Malfunctioning of the microbial loop by nutrient limitation (Thingstad et al. 1997) can be discarded in this case. In addition, it must be highlighted that cold surface waters are not the reason behind the low bacterial activity, since surface temperature during the winter survey was about the same than during the spring period. As indicated before, this is due to the entry in the ría of warm surface waters transported from subtropical latitudes by the recurrent poleward slope current observed during the winter months. This circulation pattern is also common in the other three major upwelling systems during the corresponding winter period (Bakun and Nelson 1991).

Smith and Hollibaugh (1997) studied the net ecosystem metabolism of Tomales Bay, a very small (8.4 10^{-2} km^3) and shallow (3 m deep) well–mixed estuary in the upwelling region of California, which exchanges water slowly with the adjacent shelf (flushing time, ~3 wk). For the case of DOC, they observed insignificant *NEP* rates either in the summer (maximum offshore Ekman transport) or the wintertime (offshore

Ekman transport near zero). Whereas Tomales Bay is a very particular ecosystem within the Californian upwelling, the Ría de Vigo contains a large volume of shelf waters (2.76 km^3, mean depth 20 m, flushing time ~1 wk) representative for carbon cycling in the whole Iberian upwelling system. Therefore, our results are likely representative for the other major upwelling systems of the World Ocean.

Accumulation *versus* export. hydrodynamic control of the *NEP* of DOC

Equation (13) in the 'Materials and Methods' section express numerically the possible fate of the *NEP* of labile DOC in the study ecosystem: **1**) increase the DOC standing stock, to make this labile material available to bacterial populations into the system; and/or **2**) export out of the ecosystem where the labile material was generated, to serve as new substrate for bacteria in adjacent ecosystems. The ecological implications of the two alternatives are antagonistic and they are connected to the key issue of regenerated and new production in marine systems (Eppley and Peterson 1979).

The term *NEP* has been throughoutly used in the literature as a synonymous with 'new' and 'export' production (Quiñones and Platt 1989; Hansell and Carlson 1998). Strictly speaking, *NEP* and 'new' production have the same meaning: the fraction of the total production supported by nutrients entering from the boundaries of the study ecosystem. However, *NEP* and 'export' production equals only under steady–state conditions, *i.e.* when *NEP* did not contribute to modify DOC standing stocks in the study volume. The steady–state assumption is operative when appropriate large space ($>10^{2-3}$ km) and time ($>10^{2-3}$ days) scales are considered, as for the case of global annual estimates (Walsh 1991; Wollast 1993; Hansell and Carlson 1998). However, at the short time and space scales of the present study the steady–state assumption can lead to severe misinterpretation of the ecosystem functioning.

For steady–state conditions $V \cdot \Delta DOC/\Delta t = 0$ and $NEP = O–I$. Therefore, the error associated to the steady–state assumption does not affect the qualitative interpretation of the results during the spring (Fig. 4b) and summer (Fig. 4d) surveys because of the close coupling between hydrodynamics (solid dots) and biogeochemistry (open dots) at the short–time–scale. This is the expected response when the biologically–driven recycling time of the materials produced or consumed are shorter than the hydrodynamically–driven flushing time of the study volume. Therefore, export to the adjacent ocean is the major fate of labile DOC produced under the very active wind–driven circulation pattern during summer in the Iberian margin (Haynes et al. 1993) and other coastal upwelling systems (Barber and Smith 1981; Bakun and Nelson 1991).

However, during the autumn (Fig. 4f) and winter (Fig. 4h) surveys the steady–state assumption would lead to erroneous interpretations. Consideration that the *O–I* balance express *NEP* on the study system during the autumn survey would indicate reduced biological activity in response to limited circulation during a period of wind relaxation. However, as much as +9 µmol C L^{-1} of labile DOC accumulated in the study volume during the initial 11 days and bacteria subsequently consumed them in the final 3 days. Therefore, the autumn situation is a good example of how high *NEP* at the expense of the nutrient stock accumulated in the ría is not necessarily synonymous with high export. Our transient approach allowed us to observe the time segregation between DOC phytoplankton production and subsequent *in situ* bacterial degradation.

Contrary to the autumn, wind–driven circulation was very active during the winter survey. However, reduced light–limited phytoplankton production at this time of the year precluded the intense DOC production/degradation cycle suggested by the *O–I* balance. DOC exchange across the boundaries of the study system is mainly due to

changes in the standing stock of accumulated materials with recycling time larger than the flushing time.

Implication for the carbon balance in upwelling regions

The net consumption of inorganic carbon by the community of organisms in a given system transforms into $CaCO_3$ and suspended, dissolved & sedimented organic carbon. The almost 20 years old controversy on the fate of new organic materials produced in ocean margins, horizontal export *versus in situ* oxidation, has turned around organic particles and their direct sedimentation on the shelf or export to continental slope sediments (Walsh et al. 1988; Biscaye et al. 1994). In parallel to this discussion, many marine biogeochemists centred their efforts in the minor but very reactive fraction of the DOM pool that contributes to carbon cycling in the oceans. Although the key role played by bioreactive DOM is widely recognised nowadays (e.g. Kirchman et al. 1993; Carlson et al. 1994; Hansell and Carlson 1998), it has not been properly incorporated in the discussion about the fate of organics in continental shelves. The net production of bioreactive DOM adds a new possible fate for the new production in ocean margins: the horizontal export to the adjacent ocean surface waters. This new route has to be important in coastal upwelling regions, where horizontal export is magnified by the offshore Ekman transport, specially at sites where filaments develop. In this sense, a large filament is recurrently observed off the Ría de Vigo during the upwelling season (Haynes et al. 1993). Our results indicate that ~20% of the net primary production in the study volume transform into labile DOC during upwelling episodes. This number agrees very well with the 20% value assumed by Hansell and Carlson (1998) for coastal upwelling systems of the World Ocean in their global estimates of the *NEP* of DOC.

The fate of organic materials in the global coastal upwelling zone has to be revisited under the light of these recent estimates.

Labile DOC exported to the adjacent ocean surface waters will ultimately serve as a substrate for growth and respiration of bacterial populations there. The impact of exported DOC to the activation of the microbial loop is specially important when the receptor ecosystem is oligotrophic. This is the case of the Subtropical gyres surrounding the highly productive belt of the Equatorial Pacific (Hansell and Waterhouse 1997). Therefore, horizontal export of labile DOC must also be considered in the recent controversy of the autotrophic (Williams 1998) or heterotrophic (Duarte and Agustí 1998) status of open ocean waters. Considering recent estimates (Hansell and Carlson 1998), global new production of coastal upwelling areas is 0.8 Gt C yr^{-1}. Assuming that 20% transforms into labile DOC, about 0.16 Gt C yr^{-1} could be exported from coastal upwelling systems to the adjacent open ocean waters to fuel heterotrophic processes there.

References

Álvarez–Salgado, M.D. Doval, and F.F. Pérez. 1999. Dissolved organic matter in shelf waters off the Ría de Vigo (NW Iberian upwelling system). J. Mar. Sys. 18: 383–394.

Anderson, T.R. , and P.J. Williams. 1999. A one–dimensional model of dissolved organic carbon cycling in the water column incorporating combined biological–photochemical decomposition. Global Biogeochem. Cycles 13: 337–349.

Bakun, A., and C.S. Nelson. 1991. The seasonal cycle of wind–stress curl in subtropical eastern boundary current regions. J. Phys. Oceanogr. 21: 1815–1834.

Barber, R.T., and R.L. Smith. 1981. Coastal upwelling ecosystems, p. 31–68. *In* A.R. Longhurst [ed.], Analysis of Marine Systems. Academic Press, San Diego.

Biscaye, P.E., C.N. Flagg, and P.G. Falkowski. 1994. The Shelf Edge Exchange Processes experiment, SEEP–II: an introduction to hypothesis, results and conclusions. Deep–Sea Res. 41: 231–252.

Bronk. D.A., P.M. Glibert, and B.B. Ward.1994. Nitrogen uptake, dissolved organic nitrogen release, and new production. Science 265: 1843–1846.

Carlson, C.A., H.W. Ducklow, and A.F. Michaels. 1994. Annual flux of dissolved organic carbon from the euphotic zone in the North–western Sargasso Sea. Nature 371: 405–408.

Chang, J., and E.J. Carpenter. 1985. Blooms of the dinoflagellate *Gyrodinium aureolum* in a Long Island estuary: box model analysis of bloom maintenance. Mar. Biol. 89: 83–93.

Copin–Montégut, G., and B. Avril. 1993. Vertical distribution and temporal variation of dissolved organic carbon in the North Western Mediterranean Sea. Deep–Sea Res. I 40: 1963–1972.

Cullen, J.J., S.G. Horrigan, M.E. Huntley, and F.M.H. Reid. 1982. Yellow water in La Jolla Bay, California, July 1980. I. A bloom of the dinoflagellate *Gymnodinium flavum* Kofoid and Swezy. J. Exp. Mar. Biol. Ecol. 63:67–80.

Doval. M.D., X.A. Álvarez–Salgado, and F.F. Pérez. 1997. Dissolved organic matter cycling in a temperate embayment affected by coastal upwelling. Mar. Ecol. Prog. Ser. 157: 21–37.

Duarte, C.M., and S. Agustí. 1998. The CO_2 balance of unproductive aquatic ecosystems. Science 281: 234–236

Eppley, R.W., and B.J. Peterson. 1979. Particulate organic matter flux and planktonic new production in the deep ocean. Nature 282: 677–680.

Figueiras F.G., and A.F. Ríos. 1993. Phytoplankton succession, red tides and hydrographic regime in the Rías Bajas of Galicia, p. 239–244. *In*: T.J. Smayda and Y. Shimizu [eds], Toxic Marine Phytoplankton. Elsevier, New York.

Fuhrman, J.A. 1992. Bacterioplankton roles in cycling of organic matter: the microbial food web, p. 361–383. In: P.G. Falkowski and A.D. Woodhead [eds] Primary Productivity and Biogeochemical Cycles in the Sea, Plenum Press, NY.

Hansell, D.A., and T.Y. Waterhouse. 1997. Control of the distributions of organic carbon and nitrogen in the eastern Pacific Ocean. Deep–Sea Res. I 44: 843–857.

——, and C.A. Carlson. 1998. Net community production of dissolved organic carbon. Global Biogeochem. Cycles 12, 443–453.

Haynes, R., and E.D. Barton. 1990. A poleward flow along the Atlantic coast of the Iberian Peninsula. J. Geophys. Res., 95: 11425–11441.

——, E.D. Barton, and I. Pilling. 1993. Development, persistence and variability of upwelling filaments off the Atlantic coast of the Iberian Peninsula. J. Geophys. Res. 98, 22681–22692.

Kirchman, D.L., Y. Suzuki, C. Garside, and H.W. Ducklow. 1991. High turnover rates of dissolved organic carbon during a spring phytoplankton bloom. Nature 352: 612–614.

Kirchman, D.L., C. Lancelot, M. Fasham, L. Legendre, G. Radach, and M. Scott. 1993. Dissolved organic material in biogeochemical models of the ocean, p. 209–225. *In* G.T. Evans and M.J.R. Fasham [eds]., Towards a model of Ocean Biogeochemical Processes. NATO Series I: Global Environmental Change, 10. Berlin.

Moncoiffé, G., X.A. Álvarez–Salgado, G. Savidge, and F.G. Figueiras. 2000. Seasonal and short–time–scale dynamics of microplankton community production and respiration in an inshore upwelling system. Mar. Ecol. Progr. Ser., 196: 111–126. (in press)

Nogueira, E., F.F. Pérez, and A.F. Ríos. 1997. Seasonal and long–term trends in an estuarine upwelling ecosystem (Ría de Vigo, NW Spain). Estuar. Coastal. Shelf. Sci. 44: 285–300.

Norrman, B., U.L. Zweifel, C.S. Hopkinson, and B. Fry. 1995. Production and utilisation of dissolved organic carbon during an experimental diatom bloom. Limnol. Oceanogr. 40: 898–907.

Pérez, F.F., X.A. Álvarez–Salgado, and G. Rosón. 2000. Stoichiometry of net ecosystem metabolism in coastal inlet affected by upwelling. The Ría de Arousa (NW Spain). Mar. Chem. 69: 217–236.

Quiñones, R.A., and T. Platt T. 1991. The relationship between the f–ratio and the P:R ratio in the pelagic ecosystem. Limnol. Oceanogr. 36: 211–213

Rosón, G., X.A. Álvarez–Salgado, and F.F. Pérez. 1997. A non–stationary box–model to determine residual flows in a partially mixed estuary, based on both

thermohaline properties. Application to the Ría de Arousa (NW Spain). Estuar. Coastal Shelf Sci. 44: 249–262.

Smith, S.V., and J.T. Hollibaugh. 1997. Annual cycle and interannual variability of ecosystem metabolism in a temperate climate embayment. Ecological Monographs 67: 509–533.

Thingstad, T.F., A. Hagström, and F. Rassoulzadegan. 1997. Accumulation of degradable DOC in surface waters: Is it caused by a malfunctioning microbial loop? Limnol. Oceanogr. 42: 398–404.

UNESCO. 1985. The international system of units (SI) in oceanography. UNESCO technical papers in marine sciences 45.

Walsh, J.J., P.E. Biscaye, and G.T. Csanady. 1988. The 1983–84 Shelf Edge Exchange processes (SEEP)–I experiment: hypothesis and highlights. Cont. Shelf Res. 8: 35–56.

—— 1991. Importance of continental margins in the marine biogeochemical cycling of carbon and nitrogen. Nature 359: 53–55.

Williams, P.J. 1998. The balance of plankton respiration and photosynthesis in the open oceans. Nature 394: 55–57.

Wollast, R. 1993. Interactions of carbon and nitrogen cycles in the coastal zone, p 195–210. *In* R. Wollast, F.T. Mackenzie and L. Chou [eds], Interactions of C, N, P and S Biogeochemical Cycles and Global Change. Berlin.

Wooster W.S., A. Bakun, and D.R. McClain. 1976. The seasonal upwelling cycle along the eastern boundary of the North Atlantic. J. Mar. Res. 34: 131–141.

Figure captions

Figure 1. Chart of the survey area (Ría de Vigo, Iberian Upwelling System), showing the five sampling sites distributed along the embayment. The inner (stn 1) and outer (stns 4 and 5) boundaries delimit the study system.

Figure 2. Section across the central channel of the Ría de Vigo showing the study system —with surface and bottom layer— delimited by the inner (1) and outer (4) boundaries (Fig.1). *R*+*P*–*E*, hydrological balance (continental runoff + precipitation – evaporation). *H*, heat exchange across the sea surface. Q_{B1} and Q_{B4}, bottom horizontal advective fluxes at the inner and outer boundary. Q_{S1} and Q_{S4}, surface horizontal advective fluxes at the inner and outer boundary. Sewage, advective flux from the sewage of the City of Vigo.

Figure 3. (**a**) Time course of continental runoff, *R*, and offshore Ekman transport, $-Q_X$; (**c**); salinity, (**e**) temperature, and (**g**) DOC profiles at stn 3. (**b**) Average *R*, (**d**) salinity, (**f**) temperature, and (**h**) DOC profiles along the central axes of the Ría de Vigo during the 1st sampling period: 7 to 23 April 1997. *R* in $m^3\ s^{-1}$, $-Q_X$ in $m^3\ s^{-1}\ km^{-1}$, salinity in pss, temperature in ºC, and DOC in μmol C L^{-1}.

Figure 4. Time course of cumulative water flows and DOC surface fluxes in the outer boundary of the ría during the (**a**) 1st sampling period: 7 to 23 April 1997, (**c**) 2nd sampling period: 1 to 18 July 1997, (**e**) 3rd sampling period: 15 September to 2 October 1997; (**g**) 4th sampling period: 11 to 11 December 1997. And time course of the net $O-I$ balance, the accumulation term ($V \cdot \Delta DOC/\Delta t$) and $\overline{NEP}$ term in the system during the (**b**) 1st sampling period: 7 to 23 April 1997, (**d**) 2nd sampling period: 1 to 18 July 1997, (**f**), 3rd sampling period: 15 September to 2 October 1997, (**h**) 4th sampling period: 11 to 11 December 1997. To convert kmol C into mmol C $m^{-2}\ d^{-1}$ multiply by 8.55 $10^{-3}/\Delta t$, where Δt is the corresponding time interval in days.

Figure 5. (**a**) Time course of continental runoff, *R*, and offshore Ekman transport, $-Q_X$; (**c**); salinity, (**e**) temperature, and (**g**) DOC profiles at stn 3. (**b**) Average *R*, (**d**) salinity, (**f**) temperature, and (**h**) DOC profiles along the central axes of the Ría de Vigo during the 2nd sampling period: 1 to 18 July 1997. *R* in $m^3\ s^{-1}$, $-Q_X$ in $m^3\ s^{-1}\ km^{-1}$, salinity in pss, temperature in ºC, and DOC in μmol C L^{-1}.

Figure 6. (**a**) Time course of continental runoff, *R*, and offshore Ekman transport, $-Q_X$; (**c**); salinity, (**e**) temperature, and (**g**) DOC profiles at stn 3. (**b**) Average *R*, (**d**) salinity, (**f**) temperature, and (**h**) DOC profiles along the central axes of the Ría de Vigo during the 3rd sampling period: 15 September to 2 October 1997. *R* in $m^3\ s^{-1}$, $-Q_X$ in $m^3\ s^{-1}\ km^{-1}$, salinity in pss, temperature in ºC, and DOC in μmol C L^{-1}.

Figure 7. (**a**) Time course of continental runoff, *R*, and offshore Ekman transport, $-Q_X$; (**c**); salinity, (**e**) temperature, and (**g**) DOC profiles at stn 3. (**b**) Average *R*, (**d**) salinity, (**f**) temperature, and (**h**) DOC profiles along the central axes of the Ría de Vigo during the 4th sampling period: 11 to 11 December 1997. *R* in $m^3\ s^{-1}$, $-Q_X$ in $m^3\ s^{-1}\ km^{-1}$, salinity in pss, temperature in ºC, and DOC in μmol C L^{-1}.

Table 1. Glossary of relevant terms used throughout the text.

$\overline{\beta}/\overline{\alpha}$	Average ratio of the coefficients of haline contraction and thermal expansion at the boundaries of system between 2 consecutive surveys
DOC, DOM	Dissolved organic carbon, dissolved organic matter
$\overline{DOC}_B$, $\overline{DOC}_S$	Average DOC concentration in the bottom and surface layers at the boundaries of the system between two consecutive surveys
$\overline{DOC}_R$, $\overline{DOC}_W$	Average DOC concentration in the river discharge (400 µmol C L^{-1}) and the sewage from the City of Vigo (3.6 10^3 µmol C L^{-1})
$\overline{E}$	Average evaporation between 2 consecutive surveys
ENACW	Eastern North Atlantic Central Water
$\overline{H}$	Average heat exchange flux across the air–sea interface between 2 consecutive surveys
$\overline{NEP}$	Average net ecosystem production of DOC between 2 consecutive surveys
$O-I$	Balance of DOC outputs minus inputs between 2 consecutive surveys
$\overline{P}$	Average precipitation between 2 consecutive surveys
$\overline{Q}_B$, $\overline{Q}_S$	Average bottom and surface horizontal convective water flux at the boundaries of the system between 2 consecutive surveys
$\overline{Q_B \cdot S_B}$, $\overline{Q_S \cdot S_S}$	Average bottom and surface horizontal convective salt flux at the boundaries of the system between 2 consecutive surveys.
$\overline{Q_B \cdot T_B}$, $\overline{Q_S \cdot T_S}$	Average bottom and surface horizontal convective heat flux at the boundaries of the system between 2 consecutive surveys.
$-\overline{Q}_X$	Average offshore Ekman transport between 2 consecutive surveys
$\overline{R}$	Average river water flux between 2 consecutive surveys
$\Delta S/\Delta t$, $\Delta T/\Delta t$	Changes in the salt and heat (temperature) content of the system between 2 consecutive surveys
$\overline{R \cdot T_R}$	Average river heat (temperature) flux between 2 consecutive surveys
$\overline{S_B}$, $\overline{S_S}$	Average bottom and surface salinity at the boundaries of the system between 2 consecutive surveys
$\overline{T_B}$, $\overline{T_S}$	Average bottom and surface temperature at the boundaries of the system between 2 consecutive surveys
V	Study volume of the Ría de Vigo
$\overline{w}$	Weighting factor of the relative contribution of salinity and temperature to the density gradient
$\overline{W}$	Average sewage water flux (0.5 m^3 s^{-1}) between 2 consecutive surveys

Table 2. Summary of the cumulative water flows (in km^3) and DOC fluxes (in 10^3 kmol C) in the surface and bottom, inner and outer boundaries of the Ría de Vigo (Q_{S1}, Q_{B1}, Q_{S4}, Q_{B4}), river (R) and sewage discharges during the four study periods. See Figure 2 for reference.

	Survey Period		Q_{S4}	Q_{B4}	Q_{S1}	Q_{B1}	R	**Sewage**
Spring	07–23 Apr	Water	–1.42	–1.44	0.80	0.79	$1.1\ 10^{-3}$	$0.7\ 10^{-3}$
		DOC	–114.7	–105.2	79.6	72.0	0.45	2.5
Summer	01–18 Jul	Water	4.87	4.86	0.31	0.30	$2.6\ 10^{-3}$	$0.7\ 10^{-3}$
		DOC	367.6	312.9	30.9	27.1	1.08	2.64
Autumn	15 Sep–2 Oct	Water	–0.78	–0.78	0.48	0.47	$2.3\ 10^{-3}$	$0.7\ 10^{-3}$
		DOC	–57.6	–53.3	44.3	40.8	0.92	2.64
Winter	01–11 Dec	Water	–2.36	–2.42	0.20	0.17	$15.5\ 10^{-3}$	$0.4\ 10^{-3}$
		DOC	–193.6	–192.3	17.2	13.7	6.17	1.55

Table 3. Summary of the DOC standing stocks (μmol C L^{-1}), *O–I* and *NEP* rates (mol C s^{-1}), and DOC turnover times (%d^{-1}) for the spring, summer, autumn and winter surveys. Average values for the selected time intervals described in the text for each period. The turnover time of the entire DOC pool has been calculated as $NEP \times 86400 \times 100/(DOC \times 2.76 \times 10^6)$. To convert mol C s^{-1} into mmol C m^{-2} d^{-1}, values in mol C s^{-1} have to be multiplied by $1000 \times 86400/(117\ 10^6)$. Volume of the ría: 2.76 10^9 m^3, surface of the ría 117 10^6 m^2.

	Survey period	***DOC***	***O–I***	***NEP***	**Turnover time**
Spring	07–10 Apr	77	–38.9	–49.8	–2.0
	10–23 Apr	76	–8.8	–11.1	–0.5
Summer	01–04/8–15 Jul	72	+16.8	–0.1	–0.0
	04–08/15–18 Jul	71	+53.8	+60.9	+2.7
Autumn	15–29 Sep	73	–4.2	+20.3	+0.9
	29 Sept–2 Oct	76	+24.4	–85.6	–3.6
Winter	01–05 Dec	77	+33.7	–18.6	–0.8
	05–11 Dec	76	–46.8	–10.9	–0.4

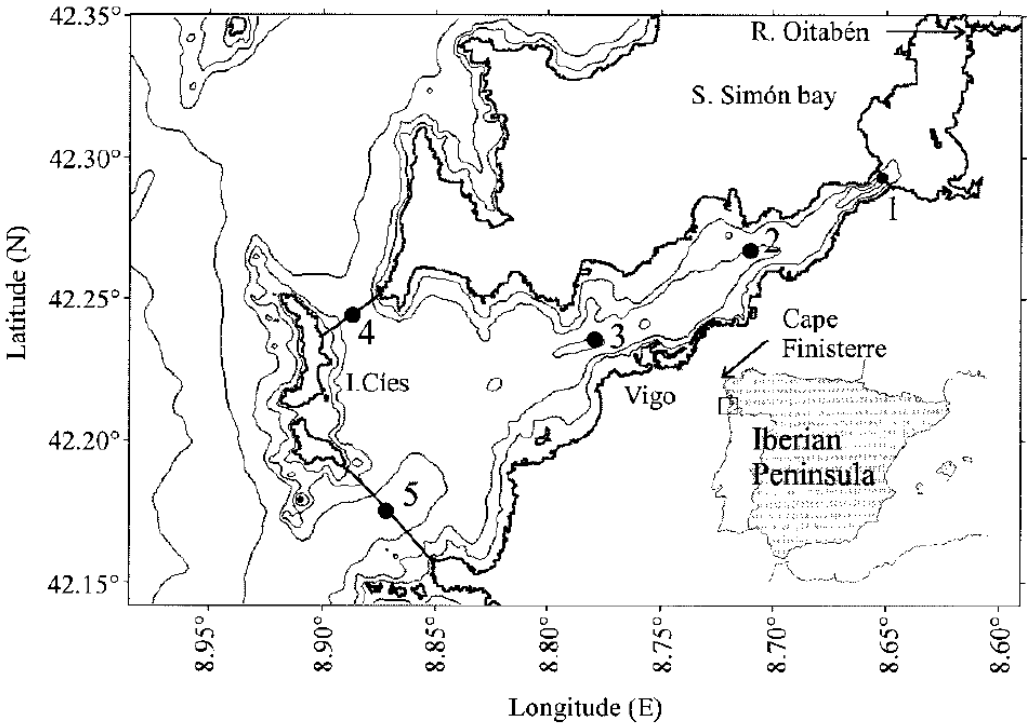

Alvarez-Salgado et al., Figure 1

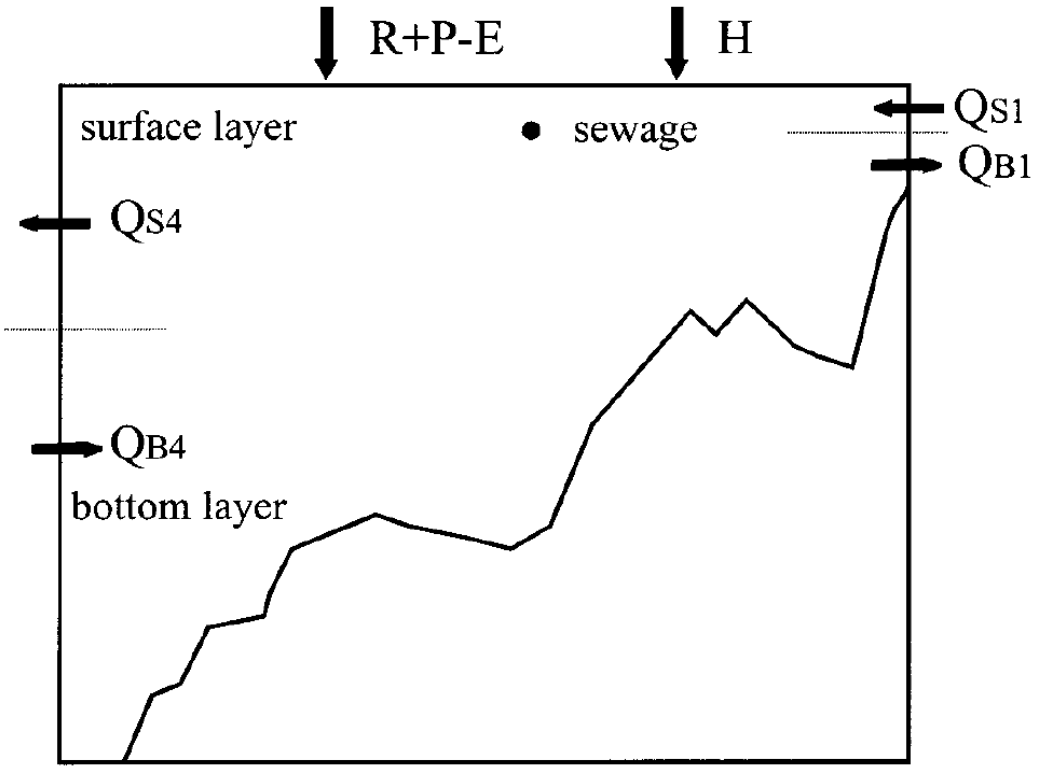

Alvarez-Salgado et al., Figure 2

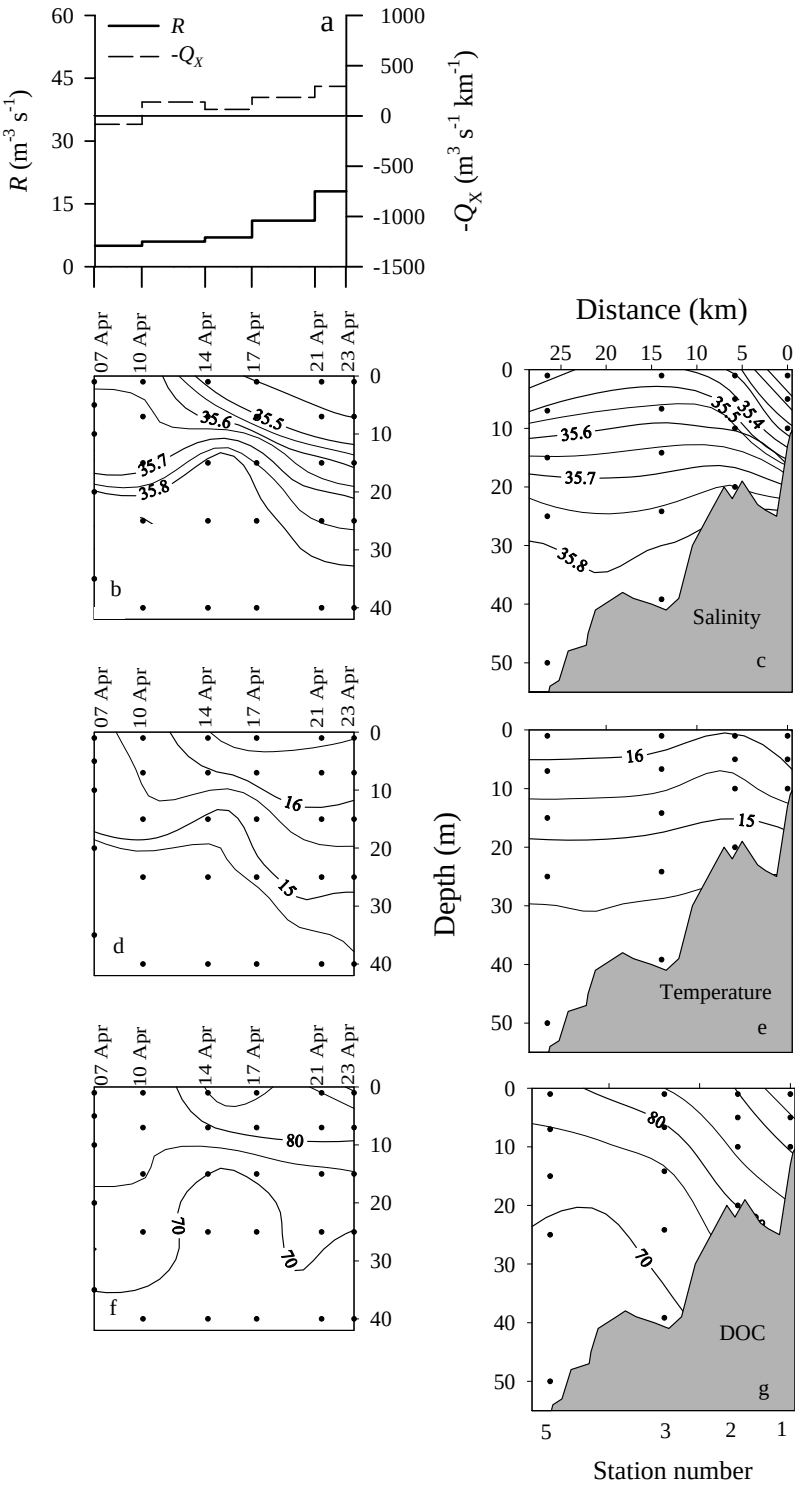

Alvarez-Salgado et al., Figure 3

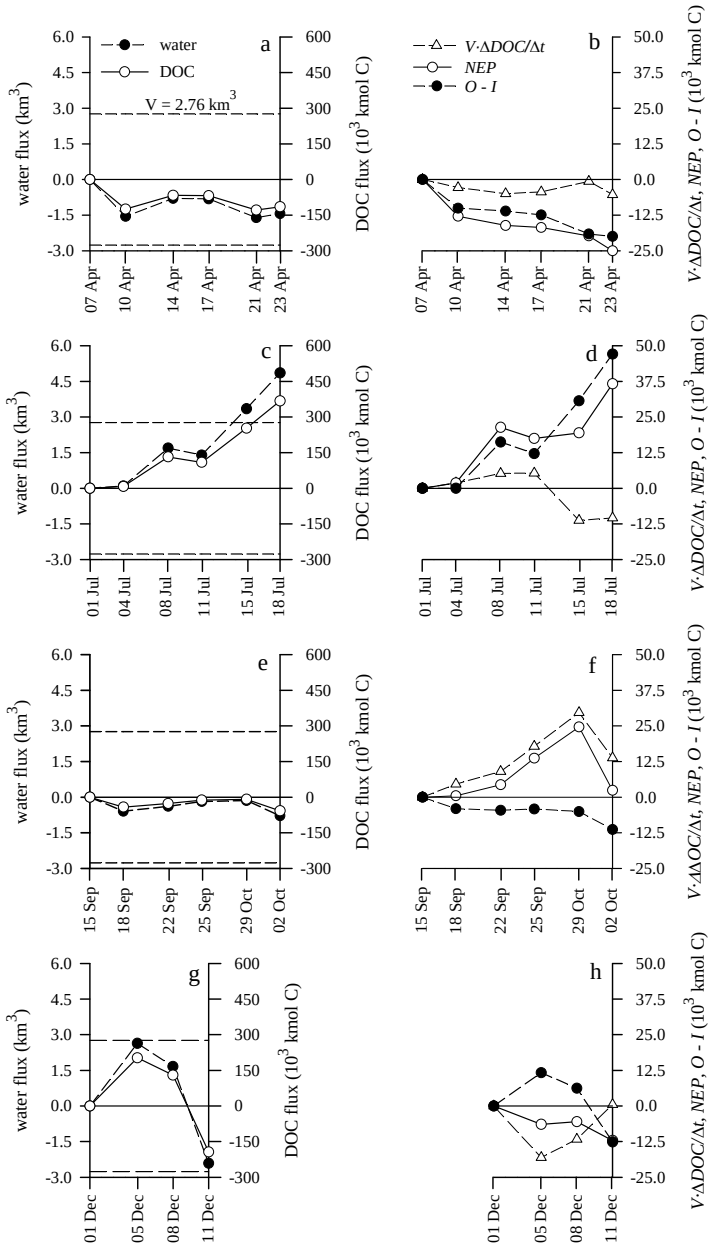

Alvarez-Salgado et al., Figure 4

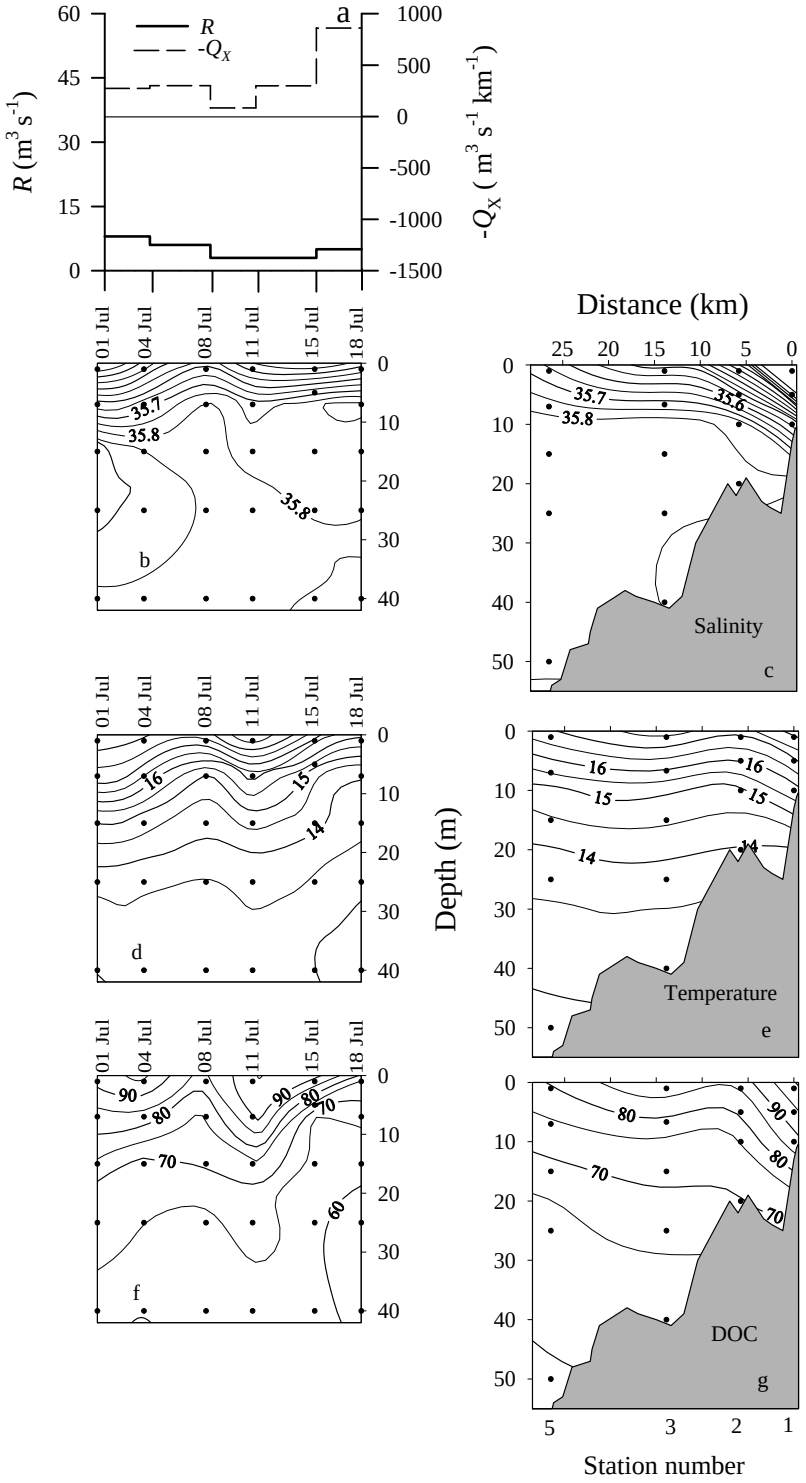

Alvarez-Salgado et al., Figure 5

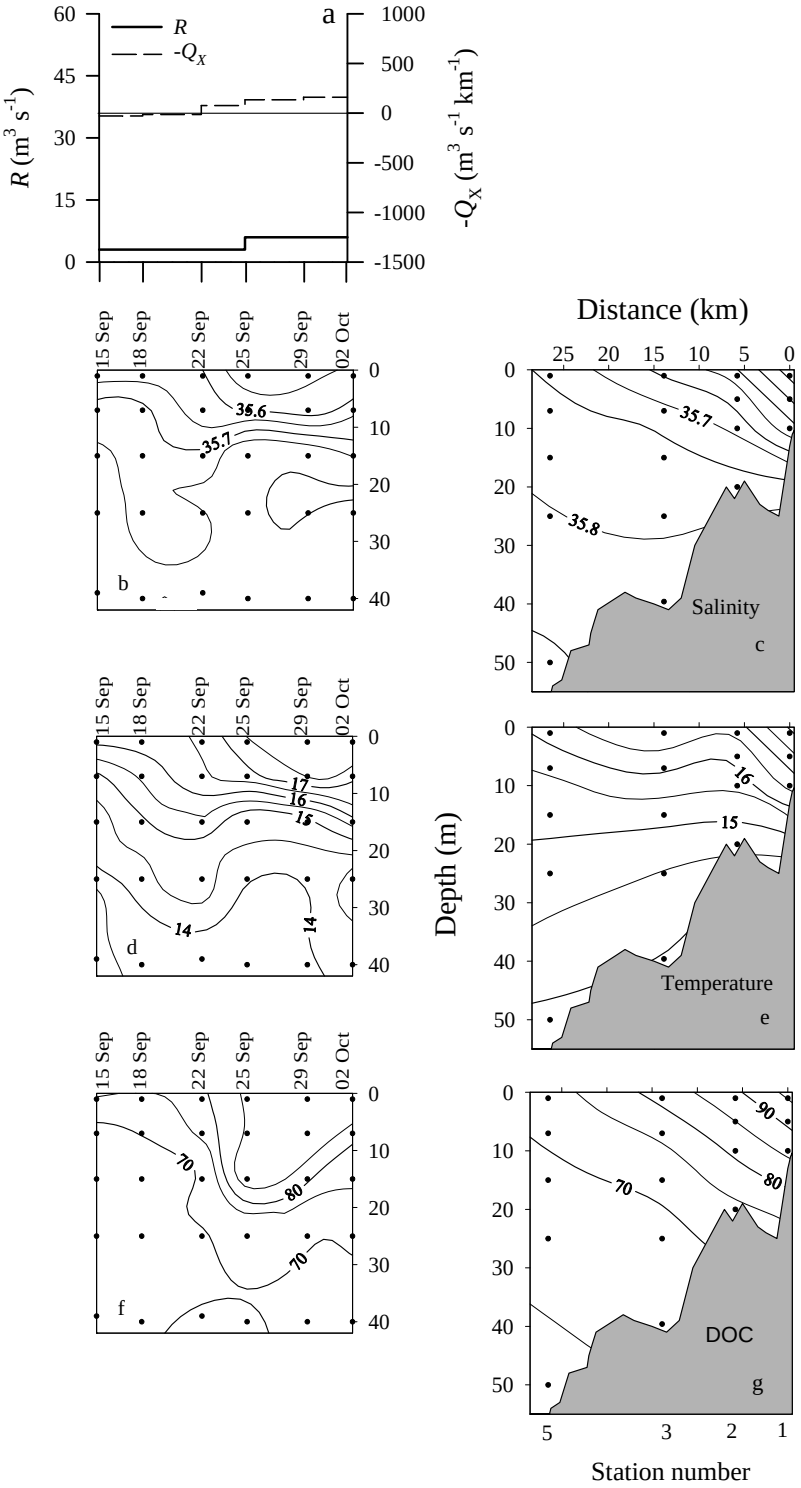

Alvarez-Salgado et al., Figure 6

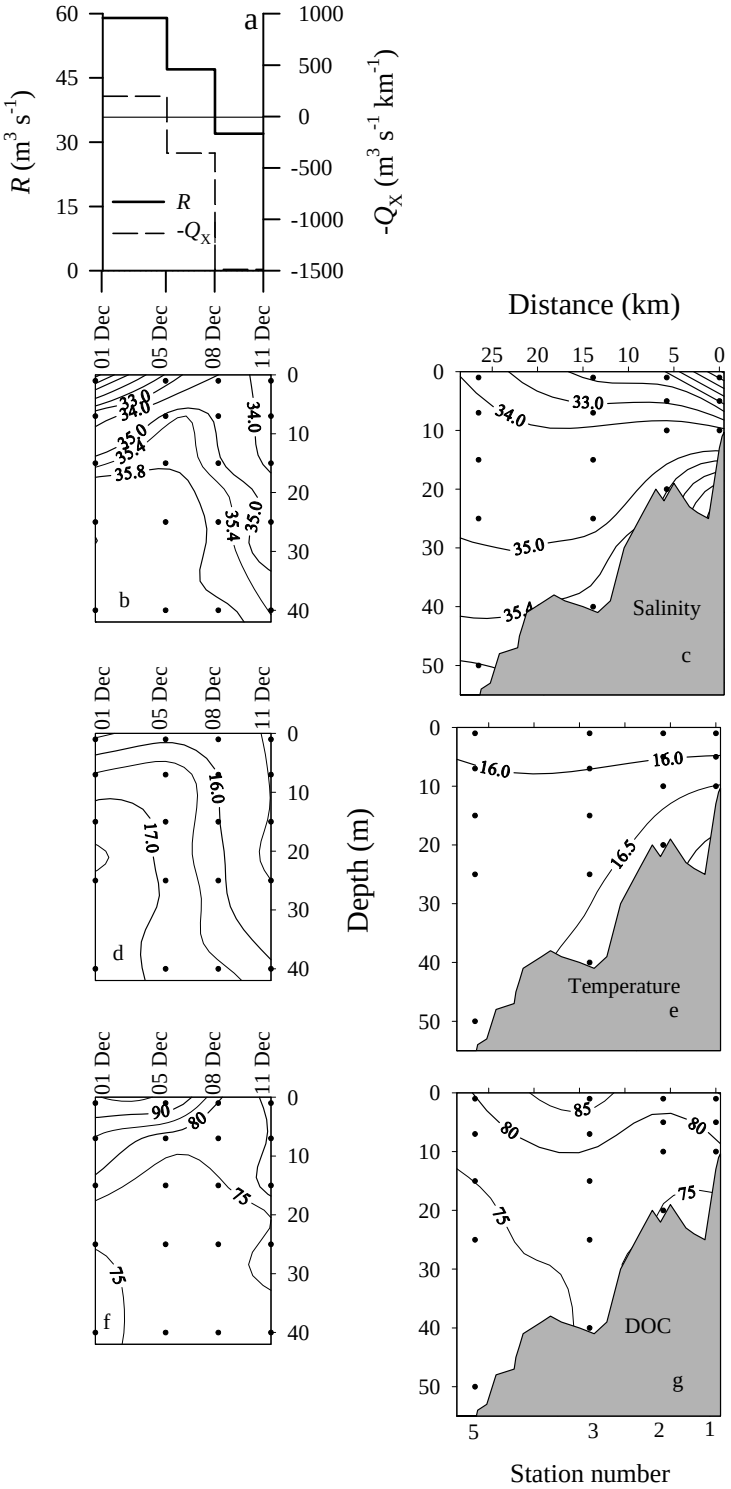

Alvarez-Salgado et al., Figure 7